## RESEARCH

# Smart textile-integrated thermochromic display for real-time temperature monitoring in elderly care

Ching Lee[1,2†], Jeanne Tan[1,2*†], Hiu Ting Tang[1,2†], Annie Yu[1], Jun Jong Tan[2], Ngan Yi Kitty Lam[1] and Ka Wing Tse[1,2]

†Ching Lee, Jeanne Tan and Hiu Ting Tang contributed equally to this work.

*Correspondence:
Jeanne Tan
jeanne.tan@polyu.edu.hk
[1]School of Fashion and Textiles, The Hong Kong Polytechnic University, Hung Hom, Kowloon, Hong Kong, China
[2]Laboratory for Artificial Intelligence in Design, Hong Kong Science Park, New Territories, Hong Kong, China

## Abstract

With the rapidly aging population, maintaining personalized thermal comfort and preventing heat loss for elderly individuals has become increasingly important. Heating textiles provide an effective solution for warmth; however, without proper monitoring, the risk of overheating in real-world applications remains a concern. To address this challenge, thermochromic textiles offer a visual, real-time temperature indication through color change, enhancing both safety and usability. In this study, thermochromic electric heating textiles were developed in woven and knitted structures, each offering distinct hand feel and performance characteristics. Key parameters, including heating efficiency, thermochromic response, thermal insulation, and overall thermal comfort, were systematically analyzed and compared. Findings reveal that double-layer fabric structures exhibit superior heat distribution and heating efficiency compared to single-layer counterparts, with the double-layer woven fabric demonstrating a more pronounced thermochromic color change upon heating. Based on these insights, a collection of thermochromic heating cushions was designed for elderly care applications. Additionally, as a proof of concept, a fully textile-based electronic control system was proposed, enabling caregivers to remotely monitor the surface temperature of the heating fabric in real time and adjust the heating levels accordingly. By bridging the fields of textile engineering, smart materials, and healthcare monitoring, this study introduces innovative design strategies that enhance both functionality and user experience in elderly-focused heating textiles.

### Article Highlights

A collection of thermochromic heating cushions for elderly care are developed in woven and knitted structures.
Double-layer woven fabric shows the highest heating efficiency and color change effect.
A textile-based control system enables real-time temperature monitoring for elderly care.

**Keywords**  Smart textile, Heating textile, Thermochromic textile, Temperature monitoring, Elderly care

## 1 Introduction

The rapid advancement of smart textile technologies has opened new possibilities for healthcare monitoring, particularly in elderly care applications. Recent studies underscore the potential of smart textiles integrated with biosensors, which can monitor physiological parameters such as heart rate, body temperature, and pressure distribution, thereby enhancing elderly individuals' comfort, safety, and overall well-being [1–4]. These innovations have led to the development of textiles designed for fall detection, cardiovascular monitoring, and thermoregulation, offering valuable real-time health insights while ensuring wearer comfort [5–11]. The relevance of elderly care as a primary application area is underscored by global demographic shifts: populations are aging rapidly in many countries, increasing demand for accessible, non-invasive health monitoring technologies to support independent and assisted living. Elderly individuals, particularly those with chronic conditions or limited mobility, are significantly more vulnerable to thermal discomfort, cold stress, or burns due to diminished thermoregulation and slower sensory response to temperature changes. However, while many of these applications focus on monitoring physiological signals, one critical area that remains less developed is thermal management through heating textiles. Despite these advancements, a significant demand still exists for textiles that provide warmth while also incorporating real-time temperature monitoring, especially for elderly individuals with reduced thermoregulatory efficiency [12–14]. In elderly care, advanced textile technologies play a crucial role in providing thermal comfort. Heating textiles have been widely employed in products such as electric blankets, heating pads, and smart garments, helping elderly users maintain an optimal body temperature and prevent cold stress [15, 16]. Yet in many current solutions, the integration of thermal feedback and user interaction remains limited or overly complex. Elderly users often experience difficulty interacting with digital displays, control panels, or mobile apps commonly paired with smart garments. Thus, an intuitive, non-intrusive feedback system becomes essential for safe, independent usage. Nevertheless, while these products are effective in delivering localized warmth, they pose significant overheating risks, particularly when continuous monitoring is unavailable [16, 17]. In settings where caregivers are responsible for regulating the heating level, insufficient feedback on surface temperature changes and the elderly individual's skin condition can lead to undesirable thermal stress, discomfort, or potential burns [17]. Therefore, integrating intelligent monitoring systems into heating textiles is essential for promoting safe and efficient usage in elderly care settings.

To address these concerns, researchers have increasingly explored passive and intuitive visualization techniques. One promising approach is incorporation of thermochromic textiles, which serve as visual indicators of temperature changes through color variation. Unlike small display screens that may be difficult for elderly individuals to read, thermochromic textiles utilize a large, fabric-based visualization method, making temperature fluctuations easier to detect by both users and caregivers. While thermochromic yarns offer an appealing, passive visual feedback mechanism that integrates naturally into textile surfaces, it is important to consider alternative approaches. Other dynamic textile display methods—such as photochromic coatings [18], electroluminescent (EL) fibers [19], and LED-integrated yarns [20]—can provide more precise, programmable, or vivid visual signals. However, these methods typically require complex circuitry, continuous power sources, or sensitivity to ambient lighting conditions, which may limit their

practical use in low-maintenance or wearable healthcare settings. In contrast, thermochromic systems consume no power during display activation and respond automatically to heat fluctuations. Despite drawbacks such as slower response time, limited repeatability, and environmental sensitivity, their simplicity and textile-conformable nature make them well-suited for non-digital, caregiver-friendly applications—especially where intuitive, low-interaction feedback is a priority. A recent study demonstrated strong potential for thermochromic yarns as visual indicators in smart heating textiles, allowing real-time, intuitive, and non-intrusive thermal feedback [21]. Another study also demonstrated that thermochromic color feedback systems, offer intuitive affordances for various user groups—especially when high-resolution or tactile-based interfaces are impractical [22]. Specifically, a smart textile that changes clothing color in response to body temperature variations associated with emotional states, enabling visual emotion recognition through localized thermochromic responses—highlighting the potential of such materials as non-verbal, ambient communication tools. While these studies primarily explore affective or emotional feedback, they reinforce the efficacy of thermally driven visual cues as context-aware, responsive textiles with opportunities for personalization. Furthermore, previous work in design for aging populations highlights the importance of multisensory and ambient feedback to compensate for declining sensory function and cognitive load [23]. Thermochromic color change aligns well with these principles by providing immediate, passive feedback that does not require digital literacy or device manipulation. In addition to thermochromic feedback, dynamic and textile-native interfaces have been explored more broadly to enhance human–fabric interactivity. For instance, user perceptions of dynamic displays embedded in garments and emphasized that non-screen-based visual feedback, such as thermochromic response or integrated textile indicators, can be more widely accepted for wearable interaction [24]. Similarly, textile-based musical controllers [25], and EmTex—an embroidered construction toolkit for responsive textile interfaces—both demonstrating the growing versatility and expressiveness of dynamic fabric technologies [26]. These prior works contextualize thermochromic textiles as part of a broader movement toward low-power, fabric-integrated interactions that promote soft, ambient, and embedded experiences. While promising, most prior studies on thermochromic textiles have concentrated on material behavior or laboratory-scale prototypes, with limited exploration of how design parameters—such as fabric structure—affect performance in real-world applications. This is particularly important for elderly users, who require solutions that are easy to interpret, reliable, and safe for unsupervised or assisted usage. Moreover, there is a lack of product-ready implementations that seamlessly integrate responsive thermal control with intuitive visual feedback in formats suitable for caregiving environments. Besides, several studies have advanced smart heating textiles through innovations in thermal control systems and energy management, limited attention has been given to the integration of thermochromic feedback as a visual indicator of surface temperature. Prior works developed an integrated control system within sandwich-structured smart textiles for active heating [27], textile-based thermal comfort systems focusing on active regulation and wearable heater integration [28], and materials and mechanisms for personal thermoregulation [29]. However, these works did not incorporate or evaluate thermochromic yarns as a passive, fabric-native means of temperature visualization. In contrast, there is a potential to combine electrical heating and thermochromic color response within

common textile structures, offering a low-power, intuitive feedback mechanism. This dual-functionality design enables not only heating but also visual monitoring, which is particularly relevant for applications where electronic interfaces may be impractical or where passive, immediate feedback is desirable. As a result, a clear gap remains in understanding the relationship between textile structure, thermochromic response, and user comfort in the context of elderly care.

Addressing this gap requires attention to both functional and tactile design aspects of smart textiles. Given the importance of sensory perception in elderly textile applications, selecting the appropriate fabric structure is essential for ensuring user acceptance. Elderly users may have different preferences regarding surface texture and hand feel, which can significantly influence their comfort and willingness to adopt new technologies [30–32]. Woven and knitted textiles, the two most commonly used textile structures, offer distinct mechanical and tactile properties. Woven fabrics, with their tightly interlaced threads, provide high durability, dimensional stability, and uniform heat distribution, making them suitable for consistent thermal performance. In contrast, knitted fabrics are characterized by softness, flexibility, and stretchability, offering a comfortable and adaptive texture, which is often preferred in contact textiles for elderly users, including those with sensory sensitivities [33, 34]. Furthermore, from an engineering perspective, textile structure also affects the alignment and density of conductive yarns, thermal buffering ability, and heat distribution pattern—all of which are crucial for balancing safety and responsiveness in heating textiles designed for continuous or long-term use. Therefore, it is necessary to systematically evaluate how different fabric structures impact not only heating efficiency but also thermochromic behavior and user-centered design requirements.

In light of these considerations, this study presents the development and characterization of thermochromic heating textiles fabricated in both woven and knitted structures. These fabrics incorporate thermochromic yarns, silver-coated conductive heating yarns, and insulating yarns, including cotton, soybean and wool, in various combinations to optimize heating efficiency, mechanical properties, and color-changing effects. Figure 1a, b illustrate the yarns used and the corresponding woven and knitted fabric structures, respectively. In this study, the thermochromic yarns function primarily as a binary visual indicator rather than as a fine-grained temperature sensor. The color transition—from purple to pink at approximately 30 °C—serves as a qualitative cue to confirm whether heating has been activated. While this single-threshold response does not provide precise or continuous temperature gradation, it offers a passive, low-energy, and textile-native method for visualizing heating status without the need for power-consuming digital displays or embedded electronics. Importantly, this color change is visible over a broad surface area, making it easily detectable by caregivers from a distance, even if the elderly user has limited visual acuity or diminished color perception. This design is intended to supplement other control mechanisms by offering a non-intrusive, intuitive cue for both users and caregivers, aligning with use scenarios such as shared caregiving settings in elder homes or hospitals. Unlike LEDs or haptic indicators, which require additional hardware and power inputs, the thermochromic mechanism integrates seamlessly into the textile structure itself, preserving comfort and wearability.

Experimental characterization revealed that double-layer structures outperformed single-layer fabrics in heat distribution and heating efficiency, with double-layer woven
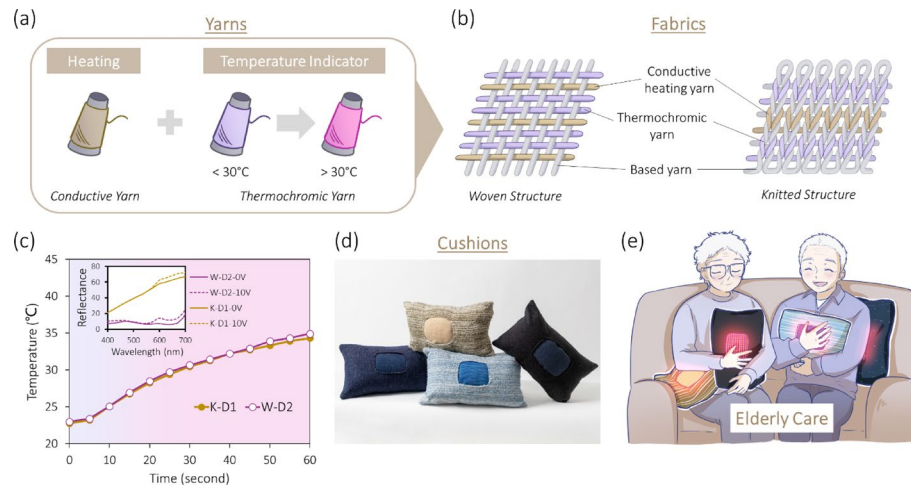
**Fig. 1** Design and development of a collection of thermochromic heating cushions using: **a** conductive yarns for heating and thermochromic yarns for temperature visualization; **b** fabrication into woven and knitted structures; **c** evaluation of heating performance and color-changing effect in double-layer woven and knitted fabrics; **d** photos of four fabricated cushions; and **e** demonstration in elderly care applications

fabrics exhibiting the most pronounced thermochromic color change upon heating. Figure 1c demonstrates the heating performance and color changes as power is supplied from 0 V (no heating) to 10 V (heating) for the double-layer knitted and woven samples, K-D2 and W-D2, respectively. As an application prototype, a collection of four thermochromic heating cushions was developed specifically for elderly care applications, as shown in Fig. 1d, e, allowing users to choose fabrics based on their preferred texture and thermal performance. Additionally, a fully textile-based electronic control system was proposed to enable caregivers to remotely monitor elderly users' skin temperature in real time and regulate the heating function accordingly. Through its interdisciplinary approach bridging textile design, smart material integration, and healthcare monitoring, this research contributes to the advancement of thermochromic smart textiles by demonstrating their practical applications in elderly care and their potential for providing safer, more intuitive, and caregiver-friendly thermal regulation.

## 2 Experimental details

### 2.1 Electrical resistance heating theory

The heating mechanism in e-textiles is primarily based on Joule heating, typically modeled using Ohmic principles as described by Ohm's Law [34–36]. When an electric current flows through a resistance—such as metallic yarns serving as bus bars and low-resistance silver- or copper-coated polymeric yarns acting as heating elements—heat is generated, resulting in a warming effect. Ohm's law could be calculated as:

$$P = VI = I^2 R \tag{1}$$

where P is the power consumption (watt), V is the voltage applied (volt), I is current (A) and R is the resistance (ohm).

Figure 2a highlights the equivalent circuit diagram of the heating fabric in both woven and knitted structures, where variables R1, R2,..., Rn represent the resistances of parallel conductive yarn strips. Additionally, variables r1, r2,..., rn and r'1, r'2,..., r'n denote pairs of contact resistances (electrodes) at left and right crossing points, respectively. To
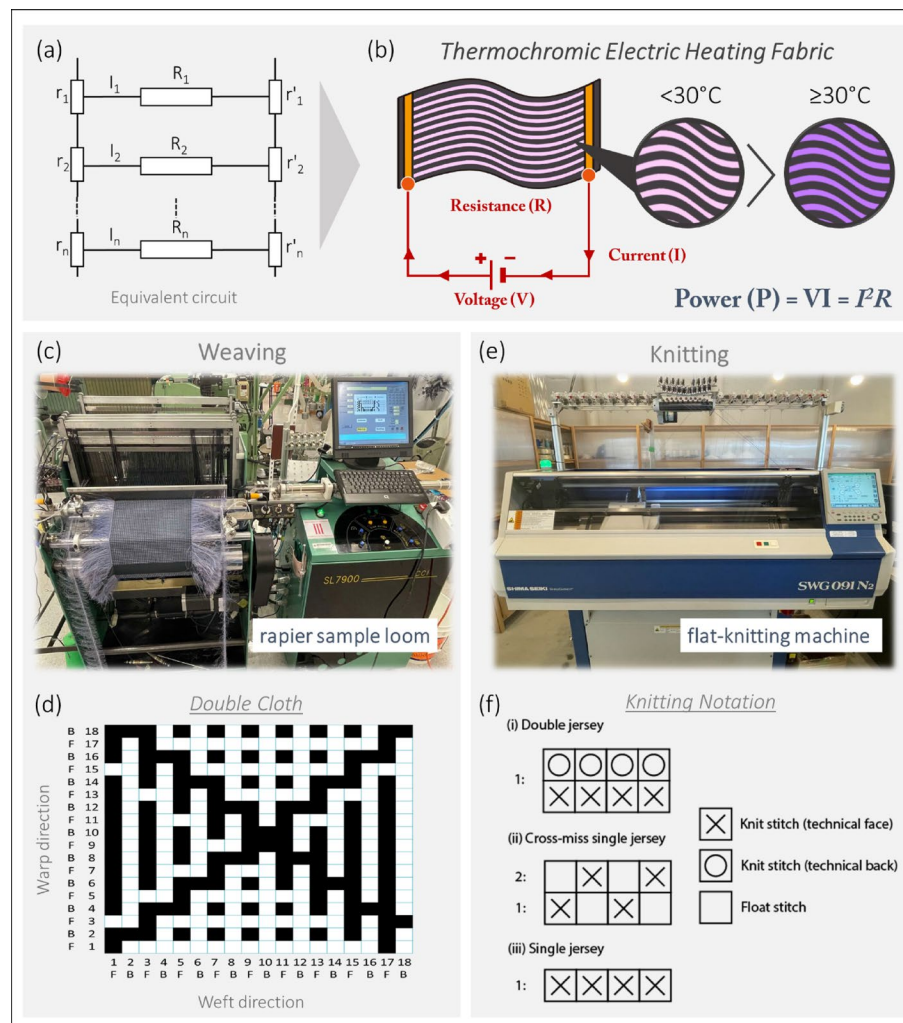
**Fig. 2** Fabrication of thermochromic electric heating fabrics: Illustration of electrical resistance heating and Ohm's Law in **a** equivalent circuit diagram and **b** color change in thermochromic yarns when heating below and above 30 °C. **c** Weaving machine and **d** Double cloth weaving structure applied. **e** Knitting machine and, **f** knitting structure of (i) double jersey, (ii) cross-miss single jersey and (iii) single jersey applied in this study

optimize thermal performance and energy efficiency, different conductive yarns were intentionally selected for the heating area and the electrode areas based on their electrical resistance. High-resistance yarns (e.g., silver-coated conductive yarns) were used in the main heating body to promote sufficient heat generation via the Joule effect. In contrast, low-resistance silver-coated conductive yarns served as electrodes or bus bars to minimize power loss and ensure uniform and efficient current delivery across the heating zone. This combination allows for targeted heat production while preserving overall electrical efficiency within the textile configuration. Figure 2b illustrates the electrical resistance heating process, in which connecting a power supply to the thermochromic electric heating fabric induces a color change from pink to purple on the surface when the temperature exceeds 30 °C. The power generated is directly proportional to the square of the current (I) and the resistance (R). In such systems, the amount of heat generated depends on the magnitude of the current, which in turn is governed by the resistance (R) and the applied voltage (V). The present study focuses exclusively on materials and textile structures exhibiting Ohmic behavior, where the current-voltage

(I–V) relationship remains linear. Non-Ohmic effects, such as those arising from material phase changes, nonlinear electrical conduction, or temperature-dependent resistance beyond the Ohmic regime, are not addressed here and remain an area for future exploration. This principle forms the fundamental operating mechanism of electric heating textiles, which typically regulate heating intensity using either direct current (DC) voltage regulation or pulse duty ratio regulation methods.
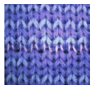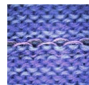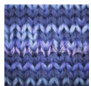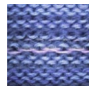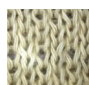
### 2.2 Fabric weaving and structure characteristics

The thermochromic heating fabric in a woven structure developed for this study was based on previous study increasing the number of conductive heating yarns enhances heating efficiency [21, 37]. The double cloth structure with a diamond pattern was chosen for its symmetry along both the vertical and horizontal axes, ensuring uniform heat distribution across each small repeat section of the fabric. The fabrication process involved weaving silver-coated heating yarn (40D, 17% silver, 83% nylon) and thermochromic yarn (150D/2) in the weft direction, while insulating passive cotton yarn (40/2s, 100% cotton) was used in the warp direction. Embroidery was applied after the weaving process to shorten the preparation time needed to replace the warp yarn with conductive yarn as a pair of electrodes. Therefore, after weaving, silver-coated yarn (200D, 18% silver, 82% nylon) was embroidered onto the fabric as electrodes, in accordance with Ohm's Law. The weaving process was carried out using a rapier sample loom (CCI/SL7900) with dobby shedding motion at a speed of 25 rpm (as shown in Fig. 2c), and the embroidery of the electrodes was done using a TAJIMA-SAI embroidery machine. Figure 2d illustrates the woven structure of the e-textile, which was fabri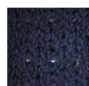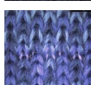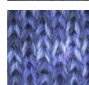cated using a double-sided diamond twill pattern. Table 1 summarizes the characteristics of the thermochromic heating fabric specimens. The fabric thickness was measured using a digital thickness gauge. Microscopic views were taken by stereo microscope (model Leica M165 C). W-D1 utilizes thermochromic yarns that changes color from grey to white, whereas W-D2 applies thermochromic yarns that changes color from pink to purple when the fabric is heated to 30 °C. Table 2 lists the specifications of the silver-coated conductive yarn. Table 3 provides the specifications of the conventional yarns used in the fabric specimens.

### 2.3 Fabric knitting and structure characteristics

Seven knitted samples of thermochromic heating fabric were fabricated. To align with the double-woven cloth, the knitted fabrics were fabricated in a double jersey structure. The fabric structure consists of two electrodes positioned along the left and right edges with a main heating area in the middle. Intarsia knitting was applied to organize the heating and electrode sections. The electrodes were knitted in a double jersey using one end of silver-coated heating yarn (800D, 17% silver, 83% nylon) with a lower resistance of 0.75 Ω/cm. One end of silver-coated heating yarn (70D, 17% silver, 83% nylon) with a higher resistance of 10.7 Ω/cm, along with one end of 150D/2 thermochromic yarn, were used to knit front stitches simultaneously in both the heating area and electrodes, forming the heating rows. Between each heating row, an interval of eight knitting rows was inserted in the heating section using textile-based yarn. Figure 2f illustrates the knitted structure of the e-textiles. K-S1 to K-S4 were knitted with single jersey for the intervals, while K-D1 to K-D3 used double jersey. Four ends of soybean yarn (40/2s,

**Table 1** Characteristics of the fabric specimens

| Sample | Microscopic image | | Fabric thickness (mm) | Area density (g/m²) | Heating area (cm²) | Insulating Yarn | Yarn density (EPI/PPI)* | Fabric resistance (Ω) | Fabric construction (Main body) |
|---|---|---|---|---|---|---|---|---|---|
| | Technical face | Technical back | | | | | | | |
| W-D1 | | | 1.48 | 540,800 | 222 | Cotton | 29/38 | 6.7 | Double Cloth |
| W-D2 | | | 1.46 | 571,400 | 227 | Cotton | 29/38 | 5.5 | Double Cloth |
| K-S1 | | | 1.21 | 441,600 | 198 | Soybean | 13/28 | 6.8 | Single Jersey |
| K-S2 | | | 1.16 | 359,200 | 178.5 | Wool | 12/34 | 10.9 | Single Jersey |
| K-S3 | | | 1.12 | 524,500 | 225 | Wool | 14.5/24 | 15.1 | Single Jersey |
| K-S4 | | | 1.43 | 647,300 | 210 | Wool | 15/23 | 11.9 | Single Jersey |
| K-D1 | | | 1.67 | 439,200 | 168 | Soybean | 13/20 | 6.7 | Double Jersey |
| K-D2 | | | 2.02 | 382,600 | 165 | Wool | 14/22 | 7 | Double Jersey |
| K-D3 | | | 2.47 | 473,900 | 206 | Wool | 13/15 | 7.7 | Double Jersey |

*Yarn density was measured on conditioned samples by using a magnifying glass to count the number of yarns in each wale and course. EPI (Ends Per Inch) refers to the yarns in the machine direction, while PPI (Picks Per Inch) represents those in the cross-direction.

**Table 2** Silver-coated conductive yarn specification

| Yarn | Fabrication | Embedded area | Yarn resistance (Ω/m) | Yarn ount (D) | End (s) | Yarn content |
|---|---|---|---|---|---|---|
| A | Weaving | Main body (Heating) | 3200 | 40 | 1 | 17% Silver, 83% Nylon |
| B | Embroidery (on woven fabric) | Electrode | 254 | 200 | 1 | 18% Silver, 82% Nylon |
| C | Knitting | Main body (Heating) | 1070 | 70 | 1 | 17% Silver, 83% Nylon |
| D | Knitting | Electrode | 75 | 800 | 1 | 17% Silver, 83% Nylon |

50% cotton, 50% soybean) were used for the interval sections in K-S1 and K-D1. For K-S2 to K-S4 and K-D2 to K-D3, the textile-based yarn used for the intervals was wool yarn (Nm 48/2, 100% extrafine merino wool), with two ends for K-S2, K-S3, and K-D2, and three ends for K-S4 and K-D3. The knitting process was performed on a computerized flat-knitting machine (Shima Seiki SWG091N2) with a gauge of 7 at a speed of 0.5 (m/s), as shown in Fig. 2e. The knitting programs were prepared using the incorporated computer-aided design system (SDS-ONE APEX).

**Table 3** Conventional yarn specification of the fabric specimens

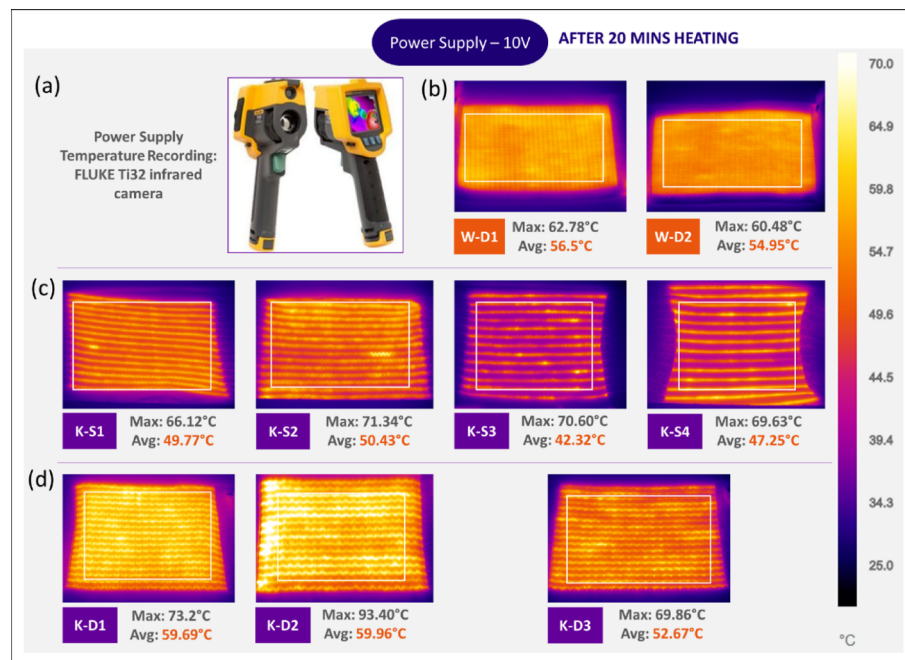| Yarn | Fabric sample | Yarn count | End(s) | Yarn content |
|---|---|---|---|---|
| Cotton | W-D1 | 40/2s | 1 | 100% Cotton |
| | W-D2 | | | |
| Soybean | K-S1 | 32s/1 | 4 | 50% Cotton |
| | K-D1 | | | 50% Soybean |
| Wool | K-S2 | NM 1/34,000 | 2 | 100% Merino wool |
| | K-D2 | | | |
| Wool | K-S3 | 48/2 Nm | 2 | 100% Merino wool |
| Wool | K-S4 | 48/2 Nm | 3 | 100% Merino wool |
| | K-D3 | | | |



**Fig. 3** Infrared (IR) tool and images of the thermochromic electric heating fabrics: **a** Thermal camera used for IR measurement. IR images of **b** woven heating fabrics (W-D1 and W-D2), **c** knitted heating fabrics structured in single jersey (K-S1 to K-S4), and **d** knitted heating fabrics structured in double jersey (K-D1 to K-D2)

### 2.4  Testing methods

### *2.4.1  Heating efficiency*

The average surface temperature of the thermochromic electric heating fabrics was monitored using a FLUKE Ti32 infrared camera (thermal sensitivity $\leq 0.05$ °C at 30 °C, resolution $320 \times 240$ pixels, image frequency 9 Hz, and calibrated temperature range $-20$ °C to 600 °C) (Fig. 3a) and a DC power supply (GPS3010D-30 V/10A). The camera was factory-calibrated with a thermal accuracy of $\pm 2$ °C or $\pm 2\%$ (whichever is greater), suitable for textile-level surface temperature analysis. Temperature readings were recorded at varying voltages and times, then analyzed through the Fluke Connect data analysis software. A multimeter (model: FLUKE 17B + digital multimeter) was used to measure the fabric's resistance. Each resistance value was recorded under static conditions (without heating) and the results showed in Table 4. Additionally, a YET-610 thermometer equipped with K-type thermocouples ($\pm 0.5$ °C accuracy) was used to collect real-time surface temperatures at four evenly spaced points. This multi-point contact method complemented the non-contact FLIR readings, ensuring validation and redundancy in

**Table 4** Summary of maximum, average, and difference in surface temperatures of thermochromic heating fabrics with corresponding fabric resistance

| Fabric sample | Max. temperature (°C) | Avg. temperature (°C) | Temperature difference (°C) | Standard Deviation (°C) | Fabric resistance (Ω) |
|---|---|---|---|---|---|
| W-D1 | 62.78 | 56.50 | 6.28 | 1.95 | 6.70 |
| W-D2 | 60.48 | 54.95 | 5.53 | 3.18 | 5.50 |
| K-S1 | 66.12 | 49.77 | 16.35 | 3.11 | 6.80 |
| K-S2 | 71.34 | 50.43 | 20.91 | 3.60 | 10.9 |
| K-S3 | 70.60 | 42.32 | 28.28 | 4.66 | 15.1 |
| K-S4 | 69.63 | 47.25 | 22.38 | 5.20 | 11.9 |
| K-D1 | 73.20 | 59.69 | 13.51 | 2.77 | 6.70 |
| K-D2 | 93.40 | 59.96 | 33.44 | 7.08 | 7.00 |
| K-D3 | 69.86 | 52.67 | 17.19 | 2.99 | 7.70 |

temperature data. Although standardized thermal testing methods (e.g., ASTM or ISO) were not applied, the experimental procedure followed established practices used in prior thermal management studies. The combination of infrared imaging, multi-point thermocouple validation, and real-time monitoring aligns with protocols reported in smart textile research [38].

### 2.4.2  Color measurement

A Datacolor 600™ Color-Eye Spectrophotometer was used due to its high precision (30 mm aperture), full visible spectrum coverage (400–700 nm), and integrated correction algorithms for glass or ambient interference. Reflectance readings at 0 V and 10 V were captured to map chromatic shifts in heated yarns. Fabric specimens were aligned in opaque form under a glass lid to ensure optical uniformity. Spectral reflectance data were collected in 10 nm intervals, capturing subtle chromatic transitions to support hue, chroma, and lightness quantification. Data were averaged from four randomized spots and directions on each sample, with optical glass correction enabled to remove any refraction effects from the container itself.

### 2.4.3  Testing for thermal conductivity, Q-max and thermal insulation.

The thermal conductivity, Q-max (a measurement of warm/cool feeling) and thermal insulation of the samples were assessed using the KES-F7 Thermo Labo II thermal property measurement instrument (Kato Tech. Co., Ltd, Japan). Prior to testing, all thermochromic electric heating fabrics were conditioned for 24 h under standard conditions of 21.1 °C ± 2 °C and 65% ± 5% relative humidity (RH). The samples were placed between the Water box (cold plate– constant temperature box) and BT-box (hot plate; area: $5 \times 5$ cm$^2$; weight: 150 g), maintained at temperatures of 30 °C ± 0.3 °C and 20 °C ± 0.3 °C, respectively. The heat flow loss W (watts) from the BT-box was recorded once a constant value was achieved. Q-max is a measurement to evaluate the instantaneous heat transfer between a fabric and the skin, indicating the warmth or coolness a material feels upon first contact. It quantifies the maximum heat flux that occurs when two surfaces at different temperatures come into contact. It can be calculated using Fourier's Law. This value is critical for elderly care applications, as the initial warm/cool feeling can directly affect user comfort perception and safety. A higher Q-max value indicates that the fabric feels cooler to the touch because it transfers heat away from the skin more quickly, while a lower Q-max value suggests the fabric retains heat, making it feel warmer. For thermal

insulation, a dry contact method was applied. Data are corrected to the value per 1 ℃ and 1 m$^2$ (The area of BT-plate is 100 cm$^2$). The thermal conductivity (k), Q-max value, and keeping warmth ratio (%) could be determined using the following equations:

$$k = \frac{W \cdot D}{A \cdot \Delta T} \tag{2}$$

$$Q_{max} = -k \cdot A \cdot \frac{\Delta T}{\Delta D} \tag{3}$$

$$\alpha = \frac{(W_0 - W)}{W_0} \times 100 \tag{4}$$

where k is the thermal conductivity, Q max is the maximum heat flux (W/m$^2$), W (watt) is the heat flow loss, D is the thickness (m) of the fabric, A is the fabric area (m$^2$) and $\Delta T$ is the temperature difference of two sides of sample, W0 is the heat loss without sample and W is the heat loss with sample.

### 2.4.4 Tensile and shear test

The tensile and shear properties were measured using the KES-FB1 Tensile and Shear Tester (Kato Tech Co., Ltd, Japan) over a vision area of 610 × 535 × 320 mm, designed to simulate mechanical stretching and in-plane displacement under low-stress textile conditions. The instrument was equipped with a 500 gf load cell, suitable for capturing deformation behavior of soft fabrics. All samples were pre-conditioned for 24 h at 21.1 ± 2 ℃ and 65% ± 5% relative humidity and cut to 20 × 20 cm dimensions for consistency. Tensile tests were performed in accordance with JIS L1096 (Japanese Industrial Standard for textile mechanical testing), using a test speed of 0.1 mm/sec, which is consistent with the low-stress mechanical testing principles adopted in the Kawabata Evaluation System. The stress–strain curve was used to determine tensile rigidity (LT), with values closer to 1 indicating greater stiffness. For shear testing, the same load cell setup and sample preparation were used. The fabrics were exposed to in-plane forces that simulate stretching and movement during wear. Measured parameters included shear rigidity (G) and low shear recovery (2HG). These values provide insights into the stability, workability, and recoverability of textile structures under small angular displacements. Testing conditions followed the KES standard protocol for shear measurements. as further detailed in related textile research studies, such as the TRJ article referenced. These measurements provide insight into how heating elements may influence the mechanical stability of dynamic textile substrates during wear or fit.

### 2.4.5 Compression test

Compression properties were assessed using the KES-FB3-A Compression Tester (Kato Tech Co., Ltd, Japan). This standard low-stress mechanical testing instrument was used to evaluate fabric compressibility, softness, and recovery characteristics through a vertically aligned plate system. The test employed a 500 gf load cell and utilized a compressive loading speed of 0.02 mm/sec, in line with testing practices defined by KES Standard Protocols and JIS L1096 recommendations for soft textile evaluation. Key metrics include compressional energy (WC), expressed in Load (gf/cm$^2$), where higher values indicate greater susceptibility to compression. Ratios such as WC/W (compressibility

per weight) and WC/T (compressibility per thickness) quantify cushioning performance, which directly ties into elderly-targeted ergonomic design.

### 2.4.6 Bending test

KES-FB2 Pure Bending Tester was applied in measuring the bending properties of fabrics, assessing the stiffness, flexibility, and drapability by applying pure bending forces without shear or tension. This method isolates bending from other deformation types, offering targeted analysis of drapability and flexibility, two key factors in assessing garment or upholstery fit. Key measurements include bending rigidity (B) and hysteresis (2HB), which reflect stiffness and recovery after bending. The B/W ratio indicates the relationship between a fabric's stiffness and weight, with higher values leading to a stiffer appearance and poor drape. The 2HB/W ratio correlates with shape instability, where a higher value means less lively movement, and 2HB/B and 2HG/G represent the balance between elastic and hysteresis components in bending and shear deformation, respectively.

### 2.4.7 Friction test

Frictional properties and surface roughness (SR) of fabrics was measured by KES-FB4-A Friction Tester which provides key insights into surface texture and tactile feel. It evaluates the coefficient of friction (MMD) and surface roughness (SMD) by passing a sensor over the fabric's surface under controlled pressure. The SR can be expressed as MMD/SMD, where the ratio of MMD (fluctuation in friction) to SMD (surface roughness) reflects the relationship between surface friction and texture. The ratio indicates surface smoothness and predict user tactile perception. A smaller ratio indicates a smoother surface, which directly correlates to how soft or smooth the fabric feels to the touch.

### 2.4.8 Air permeability test

 The KES-F8 Air Permeability Tester (Kato Tech. Co., Ltd, Japan) was used to assess the air permeability of the fabric samples by measuring their ventilation resistance. The dimensions of the test area were approximately 330 (w) × 495 (d) × 430 (h) mm. The ventilation resistance R (kPa·s/m) was recorded, with smaller values indicating higher breathability and permeability. Each sample group was tested four times, and the results were averaged to determine the fabric's overall air permeability. This parameter is important in heated textiles to ensure that thermal insulation does not overly restrict airflow, maintaining wearer comfort and thermal balance.

## 3 Results and discussion

### 3.1 Heating efficiency

Figure 3 presents the thermal images captured by a FLUKE Ti32 infrared camera with a rectangular selection within a specified area in thermal pixels, showing a temperature range from 25 to 70 °C. The images were taken after 20 min of heating with a 10 V power supply applied to the thermochromic heating fabrics. The average surface temperatures for the woven heating fabrics W-D1 and W-D2, which possess the same double cloth weaving structure, were 56.5 °C and 54.95 °C, respectively, both exhibiting uniform heat distribution in the thermal images (Fig. 3b). Table 4 shows the differences between the maximum and average temperatures were 6.28 °C and 5.53 °C for W-D1 and W-D2,

respectively. In contrast, Fig. 3c shows the thermal images for single jersey fabrics (K-S1 to K-S4) with a knitted structure, displaying several random hot spots along the conductive heating yarn. This unevenness is attributed to the inconsistent silver coating on the yarn during fabrication. When comparing the yarn materials used in the knitted structures, K-S1 and K-D1 show a relatively even heating distribution. This suggests that the soybean/cotton blended yarn provides a more stable heating distribution compared to wool. For woven heating fabrics, the tight interlacing of the structure minimizes such irregular spots, resulting in more even heat distribution. This observation is consistent with previous research showing that woven structures [39], due to their higher dimensional stability and controlled yarn alignment, support more uniform electrical pathways and energy dissipation, leading to more homogenous heating profiles. In contrast, knitted fabrics possess a looped structure with inherently higher porosity and less uniform contact between conductive fibers, facilitating the formation of localized resistive regions. These zones can result in current concentration and extreme heat formation, hence the observed hotspots and higher maximum temperatures. Compared to single jersey fabrics (K-S1 to K-S4), the double jersey fabrics (K-D1 to K-D3) shown in Fig. 3d exhibited improved heat distribution along the rows, with more courses being heated due to the increased number of silver-coated conductive yarns. However, the looped knitted structure led to loose contact between the electrodes and the heating area, causing uneven heat extraction at the intersection of the electrodes and the heating regions, particularly in K-D2, leading to extremely high temperature at 93.4 °C. Table 4 shows the differences between the maximum and average temperatures for the knitted fabrics were as follows: K-S1: 16.35 °C, K-S2: 20.91 °C, K-S3: 28.28 °C, K-S4: 22.38 °C, K-D1: 13.61 °C, K-D2: 33.44 °C, and K-D3: 17.19 °C. The difference between the maximum temperature and the average surface temperature was significantly higher in the knitted samples compared to the woven samples. This is attributed to the presence of extremely high-temperature spots on the knitted samples. Such thermal irregularities not only affect comfort levels but may also pose safety concerns in practical applications, especially in elderly care. Overall, woven structures provide more stable and even heat distribution than knitted structures in the fabrication of electric heating fabrics.

Figure 4a presents the temperature-time profiles recorded during a 60-min heating evaluation using a YET-610 thermometer equipped with thermocouples. Both woven and double jersey fabrics achieved relatively high temperatures, reaching approximately 60 °C, whereas single jersey fabrics remained below 45 °C. This result indicates that the double-layer structures accommodate more conductive heating yarns, which increases the effective pathways for electrical current and thereby enhances heat generation through Joule's effect. The presence of more conductive elements in the double-layered configuration increases the fabric's ability to convert electrical energy into thermal energy efficiently. The heating temperature of single jersey fabrics stabilized within 30 min, faster than the approximately 40 min needed for double-layer woven and double jersey samples. Figure 4b shows the relationship between electric resistance and corresponding current of each sample under a 12 V power supply. Knitted samples K-S2, K-S3, and K-S4 exhibited relatively high resistance and low current, while the woven samples showed the highest current and lowest resistance. This inverse relationship follows Ohm's Law ($I = V/R$), and clearly explains why woven fabrics, with their lower electrical resistance (e.g., ~5–6 $\Omega$), reached higher temperatures. In contrast, knitted
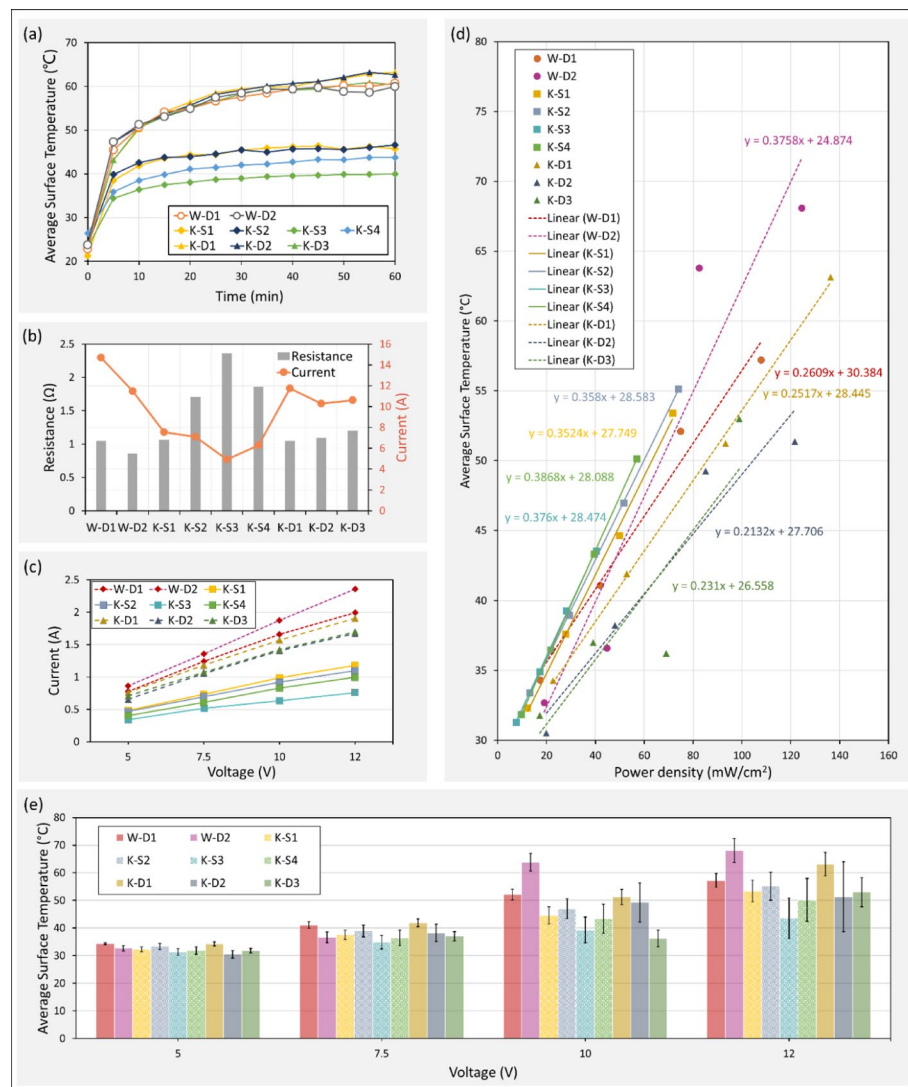
**Fig. 4** Electric heating performance of the thermochromic electric heating fabrics: **a** 60-min heating test, **b** electric resistance and current under a 12 V power supply, **c** current-voltage graph, **d** power density vs. average surface temperature curve, and **e** voltage vs. average surface temperature for all heating fabrics under 5 V, 7.5 V, 10 V, and 12 V power supplies, respectively

structures (especially single jersey samples with resistance above 10 Ω) generated less heat due to reduced current flow. Figure 4c illustrates current–voltage (I–V) profiling at input voltages of 5 V, 7.5 V, 10 V, and 12 V. All samples showed a linear increase in current with rising voltage, confirming ohmic behavior. Woven samples (W-D1 and W-D2) exhibited the highest currents, exceeding 2 A at 12 V, reflecting their superior conduction pathways. Double jersey structures followed, peaking around 1.7 A, while single jersey fabrics showed the lowest current values, approximately 1.25 A at 12 V. This pattern directly correlates with the surface temperatures observed in Fig. 4a, reinforcing that fabric structure and resistance significantly influence heating performance.

Figure 4d relates power density to average surface temperature under various voltages (5 V, 7.5 V, 10 V, 12 V), with linear trend lines plotted for each sample. All tested samples displayed positive slopes, confirming that higher power input correlates with greater surface temperatures. Among all samples, W-D2 exhibited the steepest slope,

followed by W-D1 and K-D1. This implies higher heating efficiency and power utilization in these samples under increasing energy input. Although some single jersey samples reached comparable surface temperatures to double jersey fabrics at higher voltages, they required lower power input due to limited conductive network connectivity, thus resulting in lower power density. In Fig. 4e, the average surface temperatures are presented with standard deviations indicated by error bars, obtained via infrared thermal imaging and analyzed using Fluke Connect software. At 5 V and 7.5 V, all fabrics achieved moderate temperatures of 30–35 °C and 35–40 °C, respectively, with minimal deviation across samples. At 10 V and 12 V, woven structures—particularly W-D2—performed best, recording average temperatures of 63.81 °C and 68.10 °C, approximately 10 °C higher than others, confirming their superior thermal efficiency.

Knitted fabric K-D1 also showed competitive thermal performance, but with more variation depending on the measurement method. Notably, temperature readings for K-D1 taken by thermocouples (Fig. 4a) were lower than those from IR images (Fig. 4e). This discrepancy could result from local thermal inconsistencies in the knitted structure, which are better captured by full-surface IR analysis than by point measurements, which may miss hot or cold spots. Large error bars were observed in K-D2 at 10 V and 12 V, reflecting high spatial variability in surface temperature. In contrast, K-S1 and K-D1, both incorporating soybean/cotton blend insulating yarns, demonstrated smaller error margins, similar to those observed in woven samples. This suggests that the soybean/cotton blend enhances uniform heating distribution, likely due to more consistent thermal conductivity and better integration with conductive yarns compared to wool.

### 3.2 Colorimetric effect

Figure 5 shows the microscopic view of the electric heating samples with power supplies of 0 V and 10 V, respectively, to study the color changes on the fabric surface with and without heating. Except for W-D1, where the thermochromic yarns changed from grey to white upon heating to 30 °C, the thermochromic yarns in all other samples changed from purple to pink when heated above 30 °C. In Fig. 5a, the long floats of thermochromic yarns are woven on the technical face, resulting in a more noticeable color change compared to the technical back. However, due to the structure of single-jersey knits, the long floats of thermochromic yarns appear on the technical back of the fabric (Fig. 5b). To enhance the dual-sided functionality, where the technical face provides color indication based on temperature changes and the technical back ensures comfort against the skin, double jersey fabrics were developed to conceal the thermochromic yarns from the fabric surface (Fig. 5c).

Figure 5d, e present the spectral reflectance curves for the technical face and back of the thermochromic heating fabric samples. The solid line represents fabric samples connected to 0 V (with power), while the dotted line represents samples at 10 V (without power). In Fig. 5d, which shows the technical face, the solid and dotted lines are similar in shape for all samples except W-D1, W-D2, K-S1, and K-D1. Notably, W-D2, K-S1, and K-D1 exhibit a clear reflectance gap between 600 and 700 nm (yellow, orange, and red wavelengths) due to the thermochromic yarns color change from purple to pink on the fabric surface. Additionally, W-D1 shows a distinct reflectance gap between 400 and 650 nm, indicating a shift in thermochromic yarns color from grey to white in brighter tones. In contrast, Fig. 5e shows that the reflectance gaps on the technical back side are
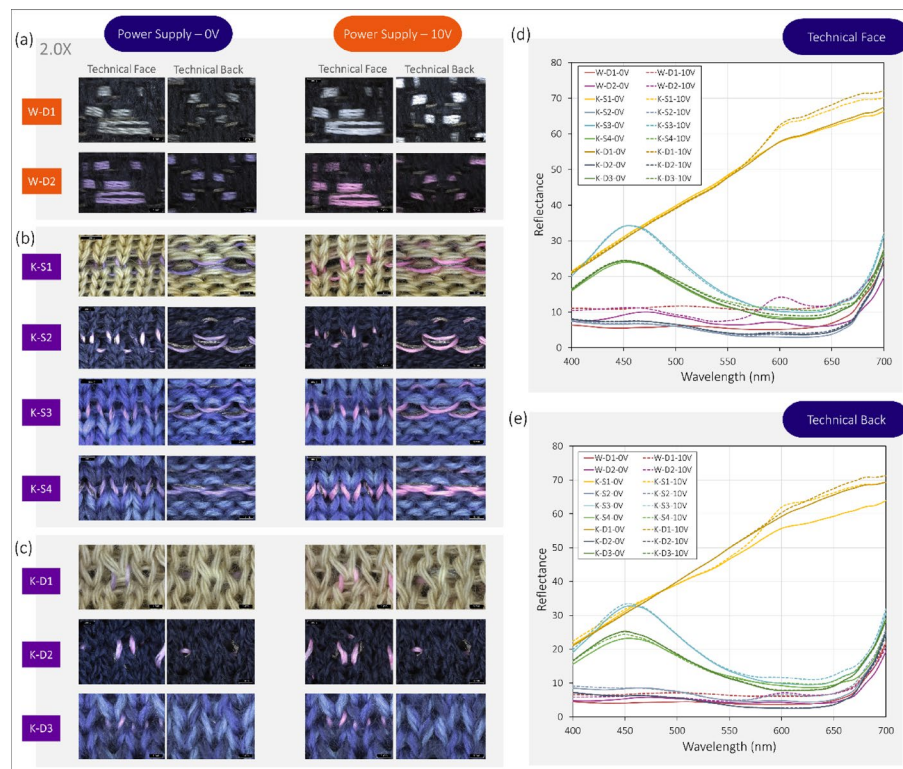
**Fig. 5** Colorimetric properties of the thermochromic electric heating fabrics: Microscopic views at 2.0× magnification of the thermochromic heating fabric in **a** woven structure, **b** single jersey knit, and **c** double jersey structure. Spectral reflectance curves for the **d** technical face and **e** technical back sides of the thermochromic heating fabric samples

much narrower, except for K-S1. These results indicate the potential of applying thermochromic yarns in woven and knitted structures for color indication. The effectiveness of thermochromic yarn's color change is influenced not only by the weaving or knitting structure but also by the insulating material. Soybean yarn (used in K-S1 and K-D1) exhibits a more noticeable color change compared to the other knitted samples, potentially due to (1) differences in base color—yellow in soybean yarn (K-S1 and K-D1) vs. blue or deep blue in wool (K-S2, K-S3, K-S4, K-D2, and K-D3)—or (2) material differences between soybean yarn and wool. Further evaluations are needed to ensure consistent material color across samples for a more standardized comparison. Standardizing the background yarn color and surface reflectivity in future work could enable more controlled comparisons of thermochromic contrast across textile structures.

In addition to the color change range, other important thermochromic performance metrics—such as the transition time (kinetics) and hysteresis—are relevant when evaluating temperature-sensitive fabric systems. This study did not quantify the time required for the color transition to initiate or complete upon heating, nor the recovery time during cooling. Kinetic behavior affects both the reaction speed and practical responsiveness in real-time monitoring applications. Furthermore, hysteresis, or the temperature difference between the 'on' and 'off' color change thresholds, could lead to uncertain visual states in fluctuating thermal environments. These factors may limit interpretability unless they are characterized and accounted for through thermal control algorithms, application constraints, or material selection. Ambient temperature fluctuations

may also influence system behavior. Since thermochromic color change occurs passively in response to heat, elevated ambient temperatures could unintentionally activate the color change, while cold environments may suppress visual transition even when heating elements are on. Future evaluations should incorporate tests under varying ambient conditions to examine environmental interference and determine the reliability of visual cues across contexts. In terms of design potential, the current use of basic double cloth and jersey architectures provides a consistent surface for thermal response but does not maximize representational or expressive capacity. Patterned or motif-based textile designs—such as shaped weaves, embroidered symbols, or differential yarn placements—could be employed to enable more meaningful visual outputs (e.g., directional arrows, icons, or heating levels). Thermochromic signals embedded into structured fabric motifs may improve user understanding and enhance usability, particularly in scenarios involving indirect observation by caregivers.

### 3.3 Thermal insulation and thermal comfort

In evaluating the physical properties under static condition without heating, since W-D1 and W-D2 share the same woven structure, only W-D2 was tested for the KES analysis. Table 5 summarizes the thermal conductivity, Q-max value, and insulation (warmth retention) ratio for one woven sample and seven knitted samples, including both single jersey and double jersey structures. The results showed that W-D2 exhibited extremely high thermal conductivity and Q-max values, but the lowest insulation ratio. Within the knitted samples, the single jersey structure demonstrated lower thermal conductivity and Q-max values when compared to the double jersey structure. Figure 6a further illustrates the thermal conductivity and insulation values. K-S1, K-D2, and K-D3 exhibited the highest insulation values, while K-S4 had the lowest. The thermal conductivity of K-S4 and K-D3 was slightly higher than the other knitted samples, and their insulation values were correspondingly lower. These findings suggest that the warmth retention effect can be optimized by increasing the density and thickness of the fabric from single jersey to double jersey, which enhances the air-trapping ability. Additionally, soybean yarn showed higher insulation values in both single jersey and double jersey structures compared to wool. These results indicate that woven structures are superior for e-textile products that require quick heat response or efficient heat transfer, such as heated blankets, battery-powered jackets, or seat warmers where the fabric needs to heat up and cool down rapidly. Conversely, knitted fabrics are better suited for thermo-insulated

**Table 5** Result in thermal conductivity, Q-max and keeping warmth ratio

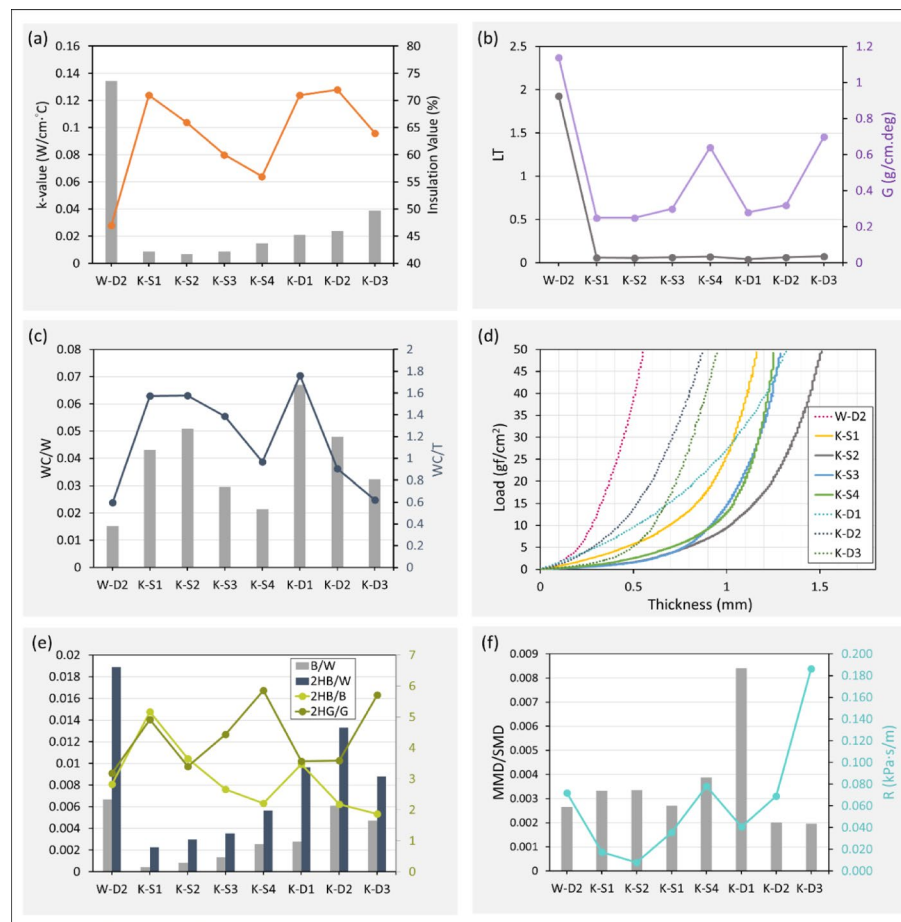| Fabric sample | Thermal conductivity (k) (W/cm °C) | Q-max value (W/cm²) | Keeping warmth ratio (α) (%) | Average heating temperature under 10 V (°C) |
|---|---|---|---|---|
| W-D2 | 0.135 | 0.087 | 47 | 54.95 |
| K-S1 | 0.009 | 0.032 | 71 | 49.77 |
| K-S2 | 0.007 | 0.029 | 66 | 50.43 |
| K-S3 | 0.009 | 0.032 | 60 | 42.32 |
| K-S4 | 0.015 | 0.029 | 56 | 47.25 |
| K-D1 | 0.021 | 0.035 | 71 | 59.69 |
| K-D2 | 0.024 | 0.034 | 72 | 59.96 |
| K-D3 | 0.039 | 0.037 | 64 | 52.67 |

**Fig. 6** Thermal insulation and thermal comfort characteristics of the thermochromic electric heating fabrics: **a** thermal conductivity and heat retention ratio, **b** tensile and shear properties, (**c** compression energy, **d** loading properties, **e** bending properties, and **f** friction and air permeability of fabric samples

garments like sweaters, socks, or base layers, where consistent warmth and comfort are critical.

Figure 6b shows the tensile and shear properties of the fabric samples. The woven sample (W-D2) exhibits the highest values in both LT (1.93) and G (1.14 g/cm deg), indicating the greatest tensile and shear rigidity among the fabric samples. In contrast, LT values for all knitted samples are relatively similar, all below 0.1. However, K-S4 and K-D3 have relatively high G values, at 0.64 g/cm.deg and 0.70 g/cm deg, respectively, compared to other knitted samples, which range from 0.25 to 0.32 g/cm.deg. This suggests that knitted wool with 3-end knitting, in both single and double structures, provides satisfactory heat retention properties. Figure 6c presents the compression results in terms of WC/W and WC/T for all fabric samples. K-D1 has the highest values, with WC/W at 0.067 and WC/T at 1.76, followed by K-S1 (0.043, 1.57) and K-S2 (0.050, 1.58). In contrast, W-D2 has the lowest values, with WC/W at 0.015 and WC/T at 0.59. Among the wool samples, the double jersey sample (K-D3) has a slightly higher WC/W value but a lower WC/T value than the single jersey samples (K-S3 and K-S4). These results suggest that the soybean yarn with a double jersey structure performs best in the compression test, indicating its potential for fabricating insulating fabrics, as higher compressibility implies better air trapping and enhanced thermal retention. Figure 6d illustrates the thickness of the
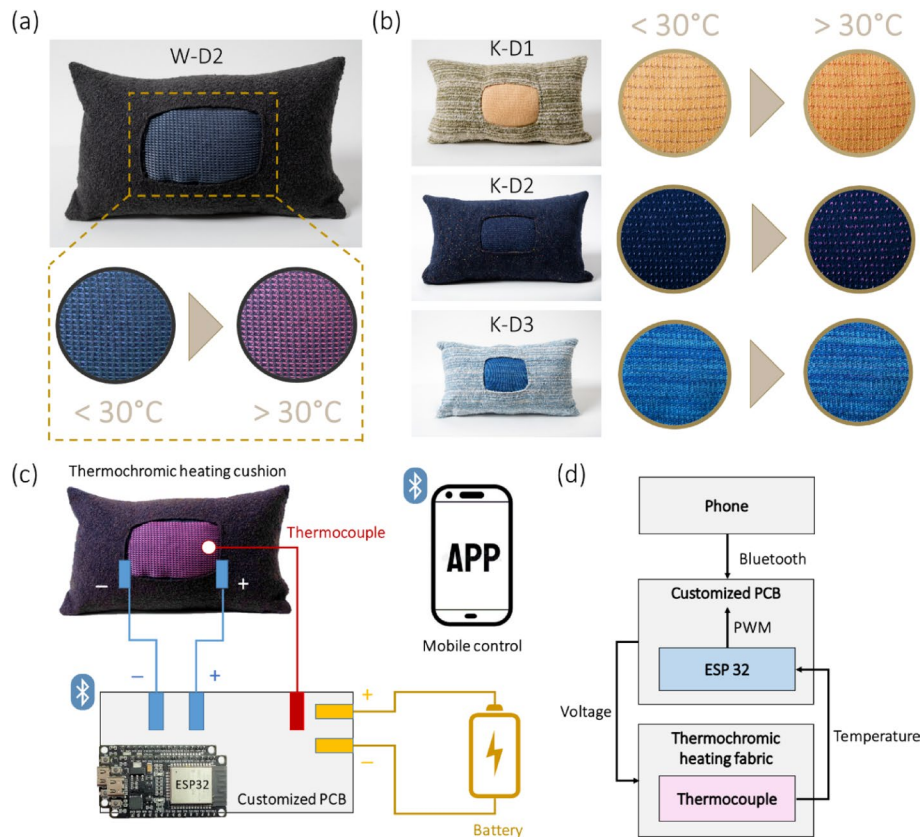
**Fig. 7** Fabrication of a collection of thermochromic heating cushions: Photos of cushions with heating sections in **a** woven and **b** knitted structures; **c** conceptual diagram; and **d** block diagram of the textile-based electronic temperature control system

fabrics under compression (at 50 gf/cm$^2$). W-D2 shows the lowest thickness (0.55), while K-S2 has the highest (1.51), highlighting that double jersey structures are generally softer than woven ones. Figure 6e demonstrates the bending properties of the fabric samples. W-D2 exhibits the highest values for B/W (0.0067) and 2HB/W (0.0189), indicating the greatest stiffness, while K-S1 shows the lowest values for B/W (0.0004) and 2HB/W (0.0023). Additionally, single-knit fabric samples tend to have lower values than double jersey ones, showing that woven structures are stiffer and less drapable, while single jersey knits offer superior flexibility. Considering shape instability, K-S4 and K-D3 exhibit the highest values for 2HG/G (5.86 and 5.71) and the lowest for 2HB/B (2.2 and 1.86), meaning they are more prone to losing shape and wrinkling during bending but have better performance in shearing. In contrast, woven fabrics, such as W-D2, with balanced values for 2HG/G (3.18) and 2HB/B (2.82), demonstrate satisfactory dimensional stability. Figure 6f displays the surface friction and air permeability characteristics of the fabric samples. Only the technical back side was tested, as the design of the thermochromic heating fabric features a face side for color indication and a back side for contact with the skin to ensure thermal comfort. K-D1 shows the highest MMD/SMD ratio (0.0084), nearly double that of other samples, which range from 0.0027 to 0.0039. A lower ratio indicates a smoother surface, so K-D1 has a rougher surface, affecting tactile comfort. In terms of breathability, K-D3 has the highest value (0.186 kPa.s/m), while K-S1 and K-S2

have the lowest values (0.017 kPa.s/m and 0.008 kPa.s/m, respectively). Smaller values indicate better breathability and permeability, so K-S2 shows poor ventilation.

### 3.4 Prototypes fabrication

A collection of thermochromic heating cushions was developed using fabrics in both woven (W-D2) and knitted structures (K-D1, K-D2, and K-D3), as shown in Fig. 6a, b, respectively. The thermochromic yarns exhibited a distinct color change from purple to pink when heated above 30 °C, with the woven fabric demonstrating the most prominent visual transformation. The cushions were designed in a practical size of 30 × 50 cm—large enough for comfort but compact enough to suit the needs of elderly users for everyday use, such as hugging or holding.

  A conceptual temperature monitoring system with Bluetooth connectivity was proposed to enable remote control of the cushion's heating function (Fig. 6c). The system integrates a thermocouple as a temperature sensor, which continuously measures the fabric's surface temperature in real time. The heating fabric and thermocouple were connected to a custom-designed printed circuit board (PCB) powered by a battery and an ESP32 microcontroller, which provides Bluetooth communication capabilities. Figure 6d illustrates the operational flow: Users adjust the desired heating level via a mobile application connected through Bluetooth. The control signal is sent to the PCB, which regulates the power supplied to the thermochromic heating fabric by adjusting the output voltage. The thermocouple simultaneously monitors the actual surface temperature. Any detected changes are transmitted to the ESP32 microcontroller. The system uses Pulse Width Modulation (PWM)—a method for controlling the amount of electrical power delivered by rapidly switching the voltage on and off—to fine-tune the heating level based on the sensed temperature. This enables real-time feedback control, ensuring the fabric stays within a safe and comfortable temperature range for the user. The system was powered by a 12 V power supply. The thermocouple sampling rate was set to 1 Hz (one reading per second), providing regular temperature updates for feedback control without overloading the microcontroller. The latency time was approximately 60 s to reach 30 °C, providing a comfortable warming effect. Regarding PWM control, no visual flickering or instability was observed in either the heating response or the thermochromic color transition. This temperature controlled based smart heating textile allows caregivers to monitor and adjust the cushion's heating level via Bluetooth, providing a safe and user-friendly interface tailored to elderly care settings. To mitigate the risk of overheating, a thermocouple is integrated into the system to provide continuous surface temperature monitoring. Conceptually, if the detected temperature exceeds a predefined threshold, the mobile application could be programmed to restrict or shut off power supply to prevent unsafe conditions. Although a single thermocouple was used in the current prototype, future iterations may incorporate multiple thermocouples across the fabric surface to ensure even temperature distribution and detect localized overheating. This data could be visualized on the mobile interface for real-time monitoring. If an extreme hotspot were to form—due to conductive yarn failure, for example—the conductive wire would likely break rapidly due to its low mechanical strength under high heat. This failure would disconnect the circuit locally and inherently prevent further heating in that area, reducing the risk of fabric ignition or skin burns.

While this prototype was developed with elderly care in mind, the underlying system architecture, which combines thermochromic color feedback, real-time temperature monitoring, and Bluetooth-enabled control, offers broader applicability across several domains. For example, similar thermochromic textiles could support safe temperature management in infant care products such as blankets or wraps, where visual cues can alert caregivers to potential overheating. In the context of sportswear, dynamic thermal feedback may assist in regulating body heat during physical activity or recovery, thereby enhancing comfort or performance. Additionally, the low-power and ambient nature of the display makes it suitable for veterinary and animal care applications, where conventional electronic interfaces may not be practical. Viewing this system as a platform for thermochromic textile interface design, rather than as a solution limited to elderly care, highlights its potential for wider use in various smart textile applications that require intuitive and passive thermal feedback.

## 4 Conclusion

This study presents the design, fabrication, and evaluation of thermochromic electric heating textiles integrated into woven and knitted fabric structures for elderly care applications. Through a comparative analysis, the thermal, colorimetric, and mechanical properties of various fabric designs were systematically assessed. The results demonstrate that double-layer woven and knitted fabrics achieve more uniform heat distribution and improved heating efficiency, with double-layer woven structures exhibiting superior heating performance, greater tensile strength, and clearer thermochromic color change. Among the insulating yarns tested, soybean–cotton blends provided more stable and uniform heating than wool-based alternatives. These findings support the tailored use of fabric structures in different applications: woven fabrics are more suitable for fast-response heating products such as blankets and seat warmers, while knitted structures are well-suited for thermo-insulated garments requiring flexibility and softness. This recommendation is based on physical and thermal performance data; however, it does not yet reflect direct user feedback. No preliminary user studies or elderly-specific trials have been conducted to assess subjective comfort, safety perception, or usability under real-world conditions. Future work will incorporate user-centered evaluations to better understand how fabric structure influences overall experience and acceptance by elderly individuals and caregivers. The development of thermochromic cushions, coupled with a textile-based electronic control system for real-time monitoring, highlights the potential of smart textiles in enhancing user safety, comfort, and caregiver convenience in elderly care. It is noted that the effect of washing on the heating performance of silver-coated yarns has not been examined in this study; as these materials may be sensitive to laundering, future research will investigate the durability and performance changes of the textiles after repeated wash cycles. Future development will also focus on extending the thermochromic response to multi-step gradients and exploring hybrid systems that incorporate additional forms of feedback (e.g., haptic or auditory) to enhance multisensory accessibility for elderly users. Incorporating user-centered design evaluations and clinical feedback is also recommended to validate thermal thresholds, visibility range, and user preferences related to thermochromic activation in the elderly context, as limited studies have evaluated thermochromic feedback specifically within elderly user groups or clinical environments—an important gap this study aims to contextualize.

Looking ahead, future research will explore the integration of voice recognition technology, supported by artificial intelligence (AI), to enable hands-free, user-friendly control of heating settings. This advancement aims to further enhance accessibility for elderly users by allowing intuitive and personalized temperature regulation through simple voice commands. Such user-centric innovations mark an important step toward the next generation of intelligent, responsive, and inclusive textile-based healthcare solutions.

**Author contributions**
Conceptualization: Ching Lee, Jeanne TanInvestigation: Ching Lee, Jun Jong TanBackground research: Ching Lee, Ka Wing TseMethodology: Ching Lee, Hiu Ting Tang, Annie Yu, Ngan Yi Kitty LamSupervision: Jeanne TanWriting– original draft: Jeanne Tan, Ching LeeWriting– review & editing: Jeanne Tan, Ching Lee, Hiu Ting TangChing Lee, Jeanne Tan, Hiu Ting Tang, these authors contributed equally to this work.All authors reviewed the manuscript.

**Data availability**
Data sets generated during the current study are available from the corresponding author on reasonable request.

## Declarations

**Ethics approval**
Not applicable.

**Consent to participate**
Not applicable.

**Consent to publish**
Not applicable.

**Competing interests**
The authors declare no competing interests.

## References

1. Ma B, Zhou Y, Tan J, Li Y, Wang X, Liu C, et al. Artificial intelligence in elderly healthcare: a scoping review. Ageing Res Rev. 2023;83:101808. https://doi.org/10.1016/j.arr.2022.101808.
2. SeyedAlinaghi S, Shokoohi M, Sahab-Negah S, Karami C, Tabatabaei A, Haghpanah S, et al. New technologies for elderly healthcare: a review of recent evidence. Public Health Environ. 2024;1(1):1–19. https://doi.org/10.70737/6t5s6w76.
3. Chaudhary B, Winnard T, Oladipo B, Das S, Matos H, et al. Review of fiber-reinforced composite structures with multifunctional capabilities through smart textiles. Text. 2024;4(3):391–416. https://doi.org/10.3390/textiles4030023.
4. Tat T, Chen G, Zhao X, Zhou Y, Xu J, Chen J, et al. Smart textiles for healthcare and sustainability. ACS Nano. 2022;16(9):13301–13. https://doi.org/10.1021/acsnano.2c06287.
5. Fan W, He J, Cai J, Li Z, Yao K, Zhang Y, et al. Machine-knitted washable sensor array textile for precise epidermal physiological signal monitoring. Sci Adv. 2020;6(11):eaay2840. https://doi.org/10.1126/sciadv.aay2840.
6. Yu A, Wang W, Li Z, Liu X, Zhang Y, Zhai J. Large-scale smart carpet for self-powered fall detection. Adv Mater Technol. 2020;5(2):1900978. https://doi.org/10.1002/admt.201900978.
7. Wicaksono I, Tucker CI, Sun T, Shi Y, Pang C, Leber KN, et al. A tailored, electronic textile conformable suit for large-scale Spatiotemporal physiological sensing in vivo. NPJ Flex Electron. 2020;4(1):1–13. https://doi.org/10.1038/s41528-020-0068-y.
8. Zhou Z, Deng Y, He Q, Yu J, Tan P, Lu B, et al. Single-layered ultra-soft washable smart textiles for all-around ballistocardiograph, respiration, and posture monitoring during sleep. Biosens Bioelectron. 2020;155:112064. https://doi.org/10.1016/j.bios.2020.112064.
9. Fang Y, Wang J, Xu Z, Pan C, Wu H. Ambulatory cardiovascular monitoring via a machine-learning-assisted textile triboelectric sensor. Adv Mater. 2021;33(41):2104178. https://doi.org/10.1002/adma.202104178.
10. Meng K, Zhao S, Zhou Y, Wu Y, Zhang S, He Q, et al. A wireless textile-based sensor system for self-powered personalized health care. Matter. 2020;2(4):896–907. https://doi.org/10.1016/j.matt.2020.02.001.
11. Rahemtulla Z, Turner A, Oliveira C, Kaner J, Dias T, Hughes-Riley T. The design and engineering of a fall and near-fall detection electronic textile. Materials. 2023;16(5):1920. https://doi.org/10.3390/ma16051920.

12.   Zhou S, Ouyang L, Li B, Hodder S, Yao R. A thermoregulation model based on the physical and physiological characteristics of Chinese elderly. Comput Biol Med. 2024;172:108262. https://doi.org/10.1016/j.compbiomed.2024.108262.
13.   Lv T, Lu Y, Zhu G. Research and analysis of user needs for smart clothing for the elderly. Wearable Technol. 2021;2:101. https://doi.org/10.54517/wt.v2i2.1653.
14.   Millyard A, Layden JD, Pyne DB, Edwards AM, Bloxham SR. Impairments to thermoregulation in the elderly during heat exposure events. Gerontol Geriatr Med. 2020;6:2333721420932432. https://doi.org/10.1177/2333721420932432.
15.   Fitriani D, Pratiwi RD, Ayuningtyas G, Murtiningsih S, Poddar S. The differences in the effectiveness of providing thick blankets and electric blankets in reducing shivering incidence on postoperative patients in surgical installations dr. Sitanala hospital tangerang, Indonesia in 2019. Malays J Med Res. 2021;5(4):28–35. https://doi.org/10.31674/mjmr.2021.v05i04.007.
16.   Liu S, Wu J. Development of user interaction (UI)-based electrically heated clothing incorporating knitted Jacquard pattern for the elderly. J Ind Text. 2024;54:15280837241287938. https://doi.org/10.1177/15280837241287938.
17.   Marius D, Rares P, Gabriella B, Liliana D, Lucian F. Georgiana lavinia R. Thermographic study on textile treatment equipment. Ann Univ Oradea Fac Text Leatherwork. 2024;25(2):87.
18.   Periyasamy A, Vikova M, Vik M. A review of photochromism in textiles and its measurement. Text Prog. 2017;49(2):53–136. https://doi.org/10.1080/00405167.2017.1305833.
19.   Lee J, Huang J, Rogers J. AC electroluminescent textiles printed with stretchable electronic inks for wearable displays. Device. 2025;2(1):22–34. https://www.cell.com/device/fulltext/S2666-9986. (25)00064-X.
20.   Chung S, Jeong S, Lee J. Highly stretchable light-emitting device for wearable displays using inorganic light-emitting diodes. Nat Commun. 2022;13(1):1057. https://www.nature.com/articles/s41467-022-28459-6.
21.   Lee C, Tan J, Tan JJ, Tang HT, Yu WS, Lam NYK. Intelligent thermochromic heating e-textile for personalized temperature control in healthcare. ACS Appl Mater Interfaces. 2025;17(3):5515–26. https://doi.org/10.1021/acsami.4c19174.
22.   Ye F, Dai J, Duan L. A novel smart textiles to reflect emotion. Int J Cloth Sci Tech. 2024;36(6):1042–54. https://doi.org/10.1108/IJCST-10-2021-0153.
23.   Umair M, Sas C, Alfaras M, ThermoPixels. Toolkit for personalizing arousal-based interfaces through hybrid crafting. In Proceedings of the 2020 ACM designing interactive systems conference. 2022; 1017–1032. https://doi.org/10.1145/3357236.3395533
24.   Devendorf L, Lo J, Howell N, Lee J, Gong N, Karagozler M, Fukuhara S, Poupyrev I, Paulos E, Ryokai K. I don't want to wear a screen: probing perceptions of and possibilities for dynamic displays on clothing. In Proceedings 2016 CHI Conference on Human Factors in Computing Systems 2016;6028–6039. https://doi.org/10.1145/2858036.2858192.
25.   Wicaksono I, Paradiso J, KnittedKeyboard. Digital knitting of electronic textile musical controllers. In Proceedings of the international conference on new interfaces for musical expression. 2020; 323–326. https://doi.org/10.5281/zenodo.4813391
26.   Wang Q, Zeng Y, Zhang R, Ye N, Zhu L, Sun X, Han T, EmTex. Prototyping Textile-Based Interfaces through An Embroidered Construction Kit. In Proceedings of the 36th Annual ACM Symposium on User Interface Software and Technology. 2023; 1–17. https://doi.org/10.1145/3586183.3606815
27.   Huang J, Li Y, Xu Z, Li W, Xu B, Meng H, et al. An integrated smart heating control system based on sandwich-structural textiles. Nanotechnology. 2019;30(32):325203.
28.   Tabor J, Chatterjee K, Ghosh T. Smart textile-based personal thermal comfort systems: current status and potential solutions. Adv Mater Technol. 2020;5(5):1901155.
29.   Fang Y, Chen G, Bick M, Chen J. Smart textiles for personalized thermoregulation. Chem Soc Rev. 2021;50(17):9357–74.
30.   Puspitosari A, Nurhidayah N. Sensory stimulation activities improving quality of life of elderly people in elderly communities. J Penelit Pendidik IPA. 2023;9(12):11038–44. https://doi.org/10.29303/jppipa.v9i12.5572.
31.   Alibakshi H, Eslami J, Shahrokhi S, Mirzabeigi H, Naimi E, Mirshoja MS. Effects of perceptual-motor exercises based on multi-sensory therapy on sensory processing of older adults. Iran J Ageing. 2024;19(3):410–23. https://doi.org/10.32598/sija.2023.2789.6.
32.   Koo J, Hwang H. Effect of sensory stimulation type on brain activity in elderly persons with mild cognitive impairment. J Int Acad Phys Ther Res. 2019;10(1):1700–05. https://doi.org/10.20540/JIAPTR.2019.10.1.1700.
33.   Jurabayev N, Shogofurov S, Kholikov K, Meliboev U. Study of the fabric structure influence on the physical-mechanical and technological properties of knitted products. E3S Web Conf. 2021;304:03030. https://doi.org/10.1051/e3sconf/202130403030.
34.   Phoophat P, Soontrunnarudrungsri A, Chollakup R. Investigation of fabric tactile characteristics for different clothing based on elderly perspectives. Suranaree J Sci Technol. 2023;30(4):0301201–9. https://doi.org/10.55766/sujst-2023-04-e02413.
35.   Xue P, Tao X, Leung MY, Zhang H. Electromechanical properties of conductive fibres, yarns and fabrics. Wearable electronics and photonics. Amsterdam: Elsevier; 2005. pp. 81–104. https://doi.org/10.1533/9781845690441.81.
36.   McBrearty D. Electronics calculations data handbook. Oxford: Elsevier; 1998.
37.   Lee C, Tan J, Tan JJ, Tang HT, Yu WS, Lam NYK. Integrating artificial intelligence for optimal thermal comfort: a design approach for electric heating textiles aligned with user preferences. Text Res J. 2025;95(5–6):513–30. https://doi.org/10.1177/00405175221148064.
38.   Woo H, Zhou K, Kim S, Manjarrez A, Hoque M, Seong T, Cai L. Visibly transparent and infrared reflective coatings for personal thermal management and thermal camouflage. Adv Funct Mater. 2022;32(38):2201432. https://doi.org/10.1002/adfm.202201432.
39.   Stoppa M, Chiolerio A. Wearable electronics and smart textiles: a critical review. Sensors. 2014;14(7):11957–92.

## Publisher's note

Springer Nature remains neutral with regard to jurisdictional claims in published maps and institutional affiliations.